BJP British Journal of Pharmacology

DOI:10.1111/bph.12051
www.brjpharmacol.org

RESEARCH PAPER

Co-expression of $Na_V\beta$ subunits alters the kinetics of inhibition of voltage-gated sodium channels by pore-blocking μ-conotoxins

Min-Min Zhang[1], Michael J Wilson[1], Layla Azam[1], Joanna Gajewiak[1], Jean E Rivier[3], Grzegorz Bulaj[2], Baldomero M Olivera[1] and Doju Yoshikami[1]

[1]*Department of Biology, University of Utah, Salt Lake City, UT, USA,* [2]*Department of Medicinal Chemistry, University of Utah, Salt Lake City, UT, USA, and* [3]*The Clayton Foundation Laboratories for Peptide Biology, The Salk Institute, La Jolla, CA, USA*

Correspondence
Professor Doju Yoshikami, Department of Biology, University of Utah, 257 South 1400 East, Salt Lake City, UT 84112, USA. E-mail: yoshikami@bioscience.utah.edu

Keywords
μ-conotoxin KIIIA; μ-conotoxin PIIIA, μ-conotoxin SmIIIA, μ-conotoxin TIIIA; $Na_V\beta$-subunit; saxitoxin, site 1; tetrodotoxin; voltage-gated sodium channel; *Xenopus* oocytes

Received
29 August 2012
Revised
19 October 2012
Accepted
24 October 2012

BACKGROUND AND PURPOSE

Voltage-gated sodium channels (VGSCs) are assembled from two classes of subunits, a pore-bearing α-subunit (Na_V1) and one or two accessory β-subunits ($Na_V\beta$s). Neurons in mammals can express one or more of seven isoforms of Na_V1 and one or more of four isoforms of $Na_V\beta$. The peptide μ-conotoxins, like the guanidinium alkaloids tetrodotoxin (TTX) and saxitoxin (STX), inhibit VGSCs by blocking the pore in Na_V1. Hitherto, the effects of $Na_V\beta$-subunit co-expression on the activity of these toxins have not been comprehensively assessed.

EXPERIMENTAL APPROACH

Four μ-conotoxins (μ-TIIIA, μ-PIIIA, μ-SmIIIA and μ-KIIIA), TTX and STX were tested against $Na_V1.1$, 1.2, 1.6 or 1.7, each co-expressed in *Xenopus laevis* oocytes with one of $Na_V\beta1$, β2, β3 or β4 and, for $Na_V1.7$, binary combinations of thereof.

KEY RESULTS

Co-expression of $Na_V\beta$-subunits modifies the block by μ-conotoxins: in general, $Na_V\beta1$ or β3 co-expression tended to increase k_{on} (in the most extreme instance by ninefold), whereas $Na_V\beta2$ or β4 co-expression decreased k_{on} (in the most extreme instance by 240-fold). In contrast, the block by TTX and STX was only minimally, if at all, affected by $Na_V\beta$-subunit co-expression. Tests of $Na_V\beta1$: β2 chimeras co-expressed with $Na_V1.7$ suggest that the extracellular portion of the $Na_V\beta$ subunit is largely responsible for altering μ-conotoxin kinetics.

CONCLUSIONS AND IMPLICATIONS

These results are the first indication that $Na_V\beta$ subunit co-expression can markedly influence μ-conotoxin binding and, by extension, the outer vestibule of the pore of VGSCs. μ-Conotoxins could, in principle, be used to pharmacologically probe the $Na_V\beta$ subunit composition of endogenously expressed VGSCs.

Abbreviations

DRG, dorsal root ganglion; INa, sodium current; μ-KIIIA, μ-conotoxin KIIIA from *Conus kinoshitai*; μ-PIIIA, μ-conotoxin PIIIA from *Conus purpurascens*; μ-SmIIIA, μ-conotoxin SmIIIA from *Conus stercusmuscarum*; μ-TIIIA, μ-conotoxin TIIIA from *Conus tulipa*; NaV1, α-subunit of voltage-gated sodium channel; NaVβ, β-subunit of voltage-gated sodium channel; NaVβ112, chimera of the extracellular and transmembrane domains of NaVβ1 and intracellular domain of NaVβ2; NaVβ211, chimera of the extracellular domain of NaVβ2 and transmembrane and intracellular domains of NaVβ1; STX, saxitoxin; TTX, tetrodotoxin; VGSC, voltage-gated sodium channel

Introduction

Voltage-gated sodium channels (VGSCs), which are responsible for the upstroke of the action potential, consist of two classes of integral membrane glycoprotein subunits, large (260 kDa) α-subunits and smaller (30–40 kDa) β-subunits. These subunits assemble into complexes formed from a single α-subunit and one or two β-subunits. Mammals have nine isoforms of the α-subunit ($Na_V1.1$ through 1.9) and four of the β-subunit ($Na_V\beta1$ through β4) (Catterall *et al.*, 2005). The α-subunit, which comprises four homologous domains, each with six membrane-spanning segments, bears the essential features of a functioning VGSC; namely, a Na^+-selective pore as well as voltage-sensors responsible for the gating of the channel in response to changes in membrane potential [for recent review see (Catterall, 2012)]. The β-subunit has a single membrane-spanning segment, with a large extracellular and small intracellular domain, and regulates the expression and trafficking of the α-subunit as well as modulates its voltage sensitivity (for recent reviews see Brackenbury and Isom, 2011; Chahine and O'leary, 2011). $Na_V\beta2$ and β4 are covalently linked to the α-subunit via a disulfide bond (Isom *et al.*, 1995a; Yu *et al.*, 2003), whereas $Na_V\beta1$ and β3 are non-covalently linked (Isom *et al.*, 1992; Morgan *et al.*, 2000). Multiple α-subunit paralogs have been found in all vertebrates examined (Lopreato *et al.*, 2001; Widmark *et al.*, 2011); and conserved orthologs of all four mammalian $Na_V\beta$ isoforms are found in fish, frog and bird, with $Na_V\beta1/\beta3$ and $Na_V\beta2/\beta4$ sharing a common ancestry (Chopra *et al.*, 2007).

Adult rat dorsal root ganglia (DRG) consist of a heterogeneous population of sensory neurons, where more than one Na_V1 and $Na_V\beta$ isoform can be expressed by a given neuron (see reviews by Dib-Hajj *et al.*, 2010; Chahine and O'leary, 2011). Thus, a given neuron may express a multiplicity of different species of VGSCs, each composed of different combinations of Na_V1 and $Na_V\beta$ isoforms, and to untangle this mélange by pharmacological means presents a challenge. We are attempting to address this problem by using conotoxins that target VGSCs, of which there are four families: μ-, μO-, δ- and ι-conotoxins. Each family has a characteristic amino acid sequence framework and distinct mode of action: μ-conotoxins are pore blockers, whereas the other three families consist of gating modifiers (Terlau and Olivera, 2004; Fiedler *et al.*, 2008; Lewis *et al.*, 2012).

We recently reported that the action potentials in A and C fibres in rat sciatic nerve could be pharmacologically dissected with a panel of μ-conotoxins, whose Na_V1 isoform selectivities were determined for $Na_V1.1$ through 1.8 expressed in *Xenopus laevis* oocytes. We concluded that mainly $Na_V1.6$ and $Na_V1.7$ were the responsible for the propagation of action potentials in A and C fibres respectively (Wilson *et al.*, 2011a). In the course of investigating the block by μ-conotoxins of TTX-sensitive sodium currents (TTX-s I_{Na}) of voltage-clamped, acutely dissociated rat dorsal root ganglion (DRG) neurons, we observed an inconsistency insofar as the kinetics of block by μ-SmIIIA of what we surmised were sodium currents mediated by $Na_V1.7$ differed between large neurons and a subset of small neurons (Zhang *et al.*, 2013). Thus, we were motivated to investigate whether association of $Na_V1.7$ with different $Na_V\beta$ subunits might account this discrepancy. In this report, we examined four TTX-sensitive

```
μ-KIIIA    ---CCN----CSSKWCRDHSRCC#
μ-SmIIIA   -ZRCCNGRRGCSSRWCRDHSRCC#
μ-PIIIA    ZRLCCGFOKSCRSRQCKOH-RCC#
μ-TIIIA    RHGCCKGOKGCSSRECROQ-HCC#
```

Figure 1

Amino acid sequences of the four μ-conopeptides used in this report. Sequences were aligned by their Cys residues, which are in bold. Z = pyroglutamine, O = hydroxyproline, # = amidated carboxyl terminal. References for sequences are as follows: μ-KIIIA (Bulaj *et al.*, 2005); μ-PIIIA (Shon *et al.*, 1998); μ-SmIIIA (West *et al.*, 2002) and μ-TIIIA (Lewis *et al.*, 2007).

Na_V1 isoforms reported to be normally present in adult rat DRG neurons, $Na_V1.1$, 1.2, 1.6 and 1.7 (Black *et al.*, 1996; 2004; Rush *et al.*, 2007; Fukuoka *et al.*, 2008), and compared how their co-expression with each of the four rat $Na_V\beta$ subunits in *X. laevis* oocytes affected their block by three conotoxins, μ-TIIIA, μ-PIIIA and μ-SmIIIA, whose sequences are illustrated in Figure 1. These conotoxins had been previously tested against $Na_V1.1$-1.8 (all from rat except $Na_V1.6$, which was from mouse) expressed in oocytes without co-expression of any $Na_V\beta$ subunit (Wilson *et al.*, 2011a). In this report, all Na_V1 subunits examined were from rat, including $Na_V1.6$, whose sensitivity to μ-conotoxins, are reported here for the first time.

Particular attention was devoted to $Na_V1.7$ because this Na_V1 isoform is implicated in the pathophysiology of inherited and acquired pain states, and antagonists of $Na_V1.7$ could serve as analgesics (Dib-Hajj *et al.*, 2009a; 2010). Only 2 of 11 μ-conotoxins recently examined blocked $Na_V1.7$ with IC_{50} or $K_d \lesssim 1$ μM: μ-SmIIIA and μ-KIIIA (Wilson *et al.*, 2011a); thus, in addition to μ-SmIIIA, μ-KIIIA was also tested on $Na_V1.7$ co-expressed with the various $Na_V\beta$ subunits. The sequence of μ-KIIIA is also illustrated in Figure 1.

We show here that co-expression of $Na_V\beta$ subunits does alter the affinities of μ-conotoxins. We believe this is the first demonstration that co-expression of $Na_V\beta$ subunits can affect the binding of a toxin that blocks VGSCs by interacting with the extracellular vestibule of the pore of the channel; that is, neurotoxin receptor site 1 (Cestèle and Catterall, 2000). Tetrodotoxin (TTX) and saxitoxin (STX), which are guanidinium alkaloids, were originally used to define site 1 (Catterall, 1980); thus, we also examined these two alkaloids and report here that their activities were minimally, if at all, altered by $Na_V\beta$ subunit co-expression. This is an interesting result to contemplate in view of our recent findings that the μ-conotoxin binding site appears to abut that of TTX and STX, but is situated more superficially in the vestibule (Zhang *et al.*, 2009; 2010a).

Methods

Toxins

μ-Conotoxins were synthesized as previously described (Wilson *et al.*, 2011a). TTX was purchased from Alomone

Labs (Jerusalem, Israel) and STX from the National Research Council of Canada (Halifax, Nova Scotia, Canada).

Cloning of rat $Na_V1.6$

Rat $Na_V1.6$ DNA (GenBank accession #NM_019266.2), subcloned in pSGEM vector (which was derived from pGEMHE vector) (Liman *et al.*, 1992), was synthesized by GenScript USA (Piscataway, NJ, USA). The DNA was amplified using the GenomiPhi V2 DNA amplification kit (GE Lifesciences, Pittsburgh, PA, USA). The amplified DNA was sequenced, digested with *Nhe*I and transcribed with T7 RNA polymerase (mMessage mMachine RNA transcription kit, Ambion, Life Technology, Grand Island, NY, USA).

The remaining clones, also from rat, were obtained as follows. $Na_V1.1$, $Na_V1.2$, $Na_V\beta1$ and $Na_V\beta2$ were provided by Prof Alan A Goldin; $Na_V\beta3$ and $Na_V\beta4$ by Prof Lori L Isom; and $Na_V1.7$ by Prof Gail Mandel. The preparation of RNA from these was as previously described (Wilson *et al.*, 2011a). The nomenclature of the channel subunits conforms to this journal's *Guide to Receptors and Channels* (Alexander *et al.*, 2011).

Construction of $Na_V\beta$ chimeras $Na_V\beta112$ and $Na_V\beta211$

We followed the lead of Zimmer and Benndorf (2002) in the construction and nomenclature of these chimeras; see also (McCormick *et al.*, 1999). Both chimeras were made by PCR. To synthesize the $Na_V\beta112$ chimera (which consisted of the extracellular and transmembrane portions of $Na_V\beta1$ and intracellular portion of $Na_V\beta2$) and the $Na_V\beta211$ chimera (which consisted of the extracellular region of β2 and the transmembrane and intracellular portions of β1), primers were designed to PCR-amplify the desired area of one subunit, followed by a 15–20 bp overhang belonging to the other subunit (designating the chimera junction; see cartoon in Figure 4B). In a subsequent PCR, the two DNA pieces were allowed to hybridize first at the overhangs and then were amplified using primers at the 5′ and 3′ ends, used to introduce restriction sites *Not*I and *Xho*I respectively. The PCR product was gel-extracted and purified using Qiaquick PCR purification kit (Qiagen Sciences, Valencia, CA, USA). The chimeras were subcloned into the pSGEM oocyte expression vector (which contains the 5′ and 3′ *Xenopus* globin regions) using the *Not*I and *Xho*I restriction sites, transformed into DH10B competent cells and grown in ampicillin-containing LB; DNA was isolated using Qiaprep Spin mini prep kit (Qiagen Sciences). The DNA was linearized using *Nhe*I, and sense RNA was transcribed using T7 polymerase (mMessage mMachine RNA transcription kit, Ambion).

Preparation and recording from X. laevis *oocytes*

Use of *X. laevis* frogs, which provided oocytes for this study, followed protocols approved by the University of Utah Institutional Animal Care and Use Committee that conform to the National Institutes of Health Guide for the Care and Use of Laboratory Animals. All studies involving animals are reported in accordance with the ARRIVE guidelines for reporting experiments involving animals (Kilkenny *et al.*, 2010; McGrath *et al.*, 2010).

Oocytes were prepared and voltage-clamped essentially as previously described (Zhang *et al.*, 2010a; Wilson *et al.*, 2011a). Briefly, a given oocyte was injected with 30–50 nl of cRNA in distilled water of one of the following rat Na_V1 isoforms without or with an equal weight of rat $Na_V\beta$ isoform cRNA (when two different $Na_V\beta$ isoforms were involved, the weight of each was equal to that of the Na_V1 isoform): $Na_V1.1$, $Na_V1.2$, $Na_V1.6$ or $Na_V1.7$ (3, 1.5, 30 or 15 ng, respectively) and incubated 1 to 6 days at 16°C in ND96 composed (in mM) of: NaCl (96), KCl (2), $CaCl_2$ (1.8) $MgCl_2$ (1) and HEPES (5), pH 7.5. The incubation medium also contained the antibiotics penicillin (100 units·mL^{-1}), streptomycin (0.1 mg·mL^{-1}), amikacin (0.1 mg·mL^{-1}) and Septra (0.2 mg·mL^{-1}). Oocytes in ND96 were two-electrode voltage-clamped using microelectrodes containing 3 M KCl (<0.5 MΩ) and clamped at a holding membrane potential of –80 mV unless indicated otherwise. Sodium channels were activated by stepping the potential to –10 mV for 50 ms every 20 s in all experiments, including toxin wash-in and washout. Current signals were filtered at 2 KHz, digitized at a sampling frequency of 10 KHz and leak-subtracted by a P/8 protocol using in-house software written in LabVIEW (National Instruments, Austin, TX, USA). All experiments were done at room temperature.

Application and washout of μ-conotoxins, TTX and STX

The oocyte-recording chamber was a 30 μL cylindrical well, 4 mm in diameter and ~3 mm deep, fabricated from the silicone elastomer, Sylgard (Dow Corning, Midland, MI). Oocytes were exposed to toxin by applying 3 μL of toxin at 10 times its final concentration with a pipettor and manually stirring the bath for a few seconds by gently aspirating and expelling a few microlitres of the bath fluid several times with the pipettor (Wilson *et al.*, 2011a). All toxin exposures were conducted in a static bath to conserve toxin. Toxins were washed out by continuous perfusion with ND96, at an initial rate of 1.5 mL·min^{-1} for 20 s, followed by a steady rate of 0.5 mL·min^{-1} (Zhang *et al.*, 2009).

Data analysis

Conductance values were calculated with the formula $g_{Na} = I_{Na}/(V_{step} - V_{rev})$, where g_{Na} is the conductance, I_{Na} is the peak current amplitude in response to the potential step, V_{step} is the test potential and V_{rev} is the reversal potential estimated by extrapolation of the linear part of the *I–V* curve at positive V_{step} values, which yielded V_{rev} values near 50 mV. Normalized activation and inactivation curves were fit to the Boltzmann equation of the form $Y = 1/(1 + \exp[(V_{step} - V_{1/2})/k])$, where Y is the normalized g_{Na} or I_{Na}, V_{step} is the test pulse (for activation curves, stepped in 5 mV increments) or the 500 ms conditioning prepulse (for inactivation curves, stepped in 10 mV increments and immediately preceded the test pulse to –10 mV), $V_{1/2}$ is the voltage at half-maximal activation or inactivation and k is the slope factor. Fits of activation and inactivation curves to the Boltzman equation were obtained with Prism software (GraphPad Software Inc., San Diego, CA, USA).

Fitting of time course data to a single-exponential function was done with home-made software written with LabVIEW (e.g. to obtain rates of fast inactivation from the falling phases of current traces).

The interaction of toxin with channel was assumed to be that of simple bimolecular reaction whose kinetics are

described by the following equation: $k_{obs} = k_{on}[toxin] + k_{off}$, with kinetic constants determined as previously described (West *et al.*, 2002). Briefly, the time course of peak I_{Na} was plotted before, during and after exposure to toxin. The rate constant for the recovery from block, k_{off}, was determined by fitting the toxin-washout curve to a single-exponential function. However, when recovery from block was very slow (less than 50% recovery after 20 min), k_{off} was estimated from the level of recovery observed after 20 min of washing and assuming recovery followed a single-exponential time course; these involved k_{off} values <0.035·min^{-1} (Zhang *et al.*, 2009; Wilson *et al.*, 2011a). Values of k_{off} are presented as the mean obtained with $n \geq 9$ oocytes. Times longer than 20 min were not used to avoid error due to drift in baseline.

The onset of block was fit to a single-exponential function to yield the observed rate constant, k_{obs}. Values of k_{obs} were determined for at least three toxin concentrations (where each concentration was tested with at least three different oocytes) and plotted as a function of [toxin], the slope of the linear regression fit yielded k_{on}. In principle, the *Y*-intercept of this plot should yield k_{off}, but we chose to calculate k_{off} directly from toxin-washout curves (see above) to avoid extrapolation errors. The dissociation constant, K_d, was calculated from the ratio k_{off}/k_{on}. In instances where the level of block achieved a steady state within the experimental time frame of ~20 min, steady-state dose–response curves were fit to the equation: % block = 100% × (1/(1 + (IC_{50}/[toxin]))), and IC_{50} values were obtained using either Prism software or KaleidaGraph (Synergy Software, Reading, PA). When a toxin blocked very poorly (i.e. less than half-block was achieved at the highest toxin concentration tested), K_d was estimated from the level of block (% block) achieved at the highest [toxin] tested by use of the Langmuir adsoption isotherm: % block = 100% × (1/(1 + (K_d/[toxin]))).

The tests of co-expression with each the four Na$_V$β subunits yielded a large set of kinetic data, which was condensed to Δ*k* values as follows. The relative change in a kinetic rate constant (either k_{on} or k_{off}) induced by co-expression of a Na$_V$β subunit, Δ*k*, was the ratio $A \times (k^+/k^-)$, where k^+ and k^- are the respective rates with and without Na$_V$β subunit co-expression, and $A = 1$ or -1 when Na$_V$β subunit co-expression increased *k* or decreased *k* respectively. Thus, a positive Δ*k* indicates the factor by which Na$_V$β subunit co-expression increased the rate constant, and a negative Δ*k* indicates the factor by which Na$_V$β subunit co-expression decreased the rate constant.

Data are represented as mean ± SE. Statistical comparisons were performed by two-tailed unpaired *t*-tests, except for k_{on} values, where analysis of covariance was performed with Prism software.

Results

All VGSCs examined in this report were those exogenously expressed in oocytes. The intrinsic biophysical properties of α-subunits are altered by co-expression with the various Na$_V$β subunits, and we will first consider this aspect of Na$_V$β subunit co-expression before presenting results regarding the influence Na$_V$β subunit co-expression exerted on the pharmacological properties of VGSCs.

Na$_V$β subunits and the biophysical properties of sodium currents in oocytes exogenously expressing Na$_V$1.7

Rat Na$_V$β1 through β4 were individually co-expressed with rat Na$_V$1.7 in oocytes, which were two-electrode voltage clamped to measure voltage-gated sodium currents (I_{Na}) as described in Methods. Figure 2A shows representative current traces, and the effects of Na$_V$β subunit co-expression on the voltage dependence of activation and inactivation are plotted in Figure 2B. The biophysical parameters are quantified in Table 1, which shows that at least two of the five parameters were significantly changed by co-expression of each of Na$_V$β2 and β4, whereas all five parameters were significantly changed by co-expression of each of Na$_V$β1 and β3. The effects of the latter largely mirrored each other; that is, both Na$_V$β1 and β3 co-expression decreased the time constant of fast inactivation three- to fourfold and shifted the $V_{1/2}$ of activation and inactivation by about –10 and –5 mV respectively (Table 1). The effects of co-expression of Na$_V$β1 with

Table 1

Activation and inactivation parameters and time constants of fast inactivation of Na$_V$1.7 without and with Na$_V$β-subunit co-expression

	Activation[a]		Inactivation[b]		Inactivation[c]
Na$_V$1.7	**$V_{1/2}$ (mV)**	**k (mV)**	**$V_{1/2}$ (mV)**	**k (mV)**	**τ (ms)**
Alone	–10.5 ± 0.3	7.2 ± 0.3	–59.4 ± 1.1	–14.4 ± 1.0	6.1 ± 0.6
+β1	–20.0 ± 0.3*	4.8 ± 0.3*	–64.7 ± 0.4*	–8.2 ± 0.3*	2.1 ± 0.2*
+β2	–9.9 ± 0.3	5.2 ± 0.2*	–60.2 ± 0.9	–10.9 ± 0.8*	6.0 ± 0.3
+β3	–19.1 ± 0.2*	4.8 ± 0.2*	–66.1 ± 0.4*	–7.2 ± 0.4*	1.5 ± 0.2*
+β4	–23.2 ± 0.2*	5.3 ± 0.2*	–59.5 ± 0.6	–11.1 ± 0.5*	6.2 ± 0.3

[a]Data from Figure 2B, left.
[b]Data from Figure 2B, right.
[c]Time constant of fast inactivation from falling phase of I_{Na}, in response to voltage step to –10 mV (see e.g. Figure 2A), fit to a single-exponential function ($n \geq 6$ oocytes).
*Statistically different from Na$_V$1.7 expressed alone ($P < 0.05$).

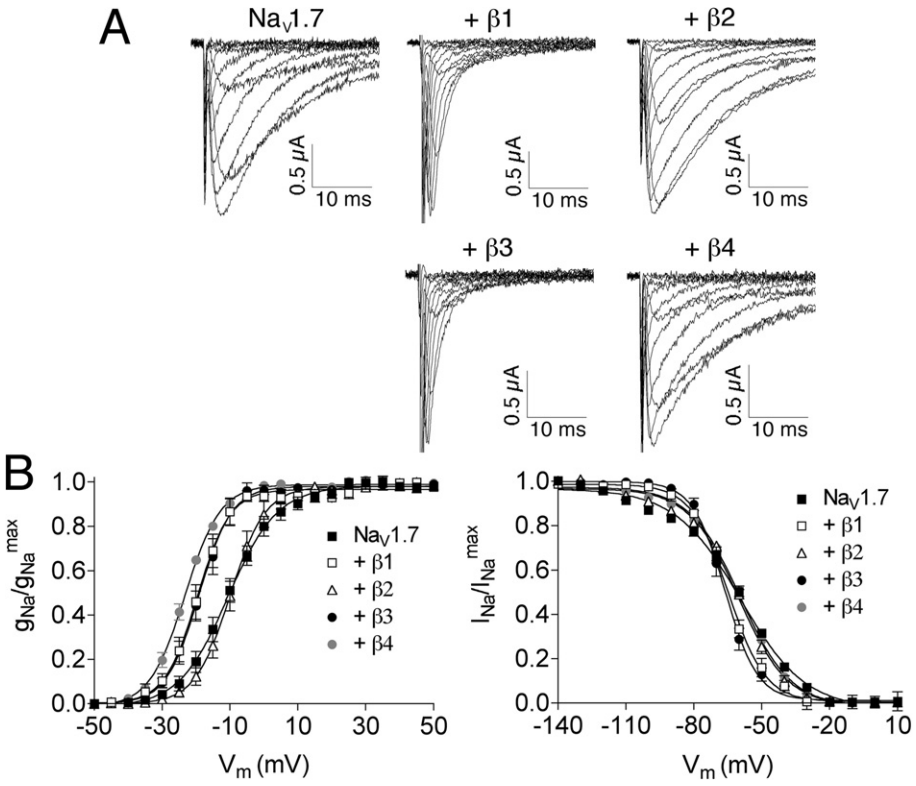

Figure 2

Sodium current traces and activation and inactivation curves of Na$_V$1.7 without and with co-expression of Na$_V$β1, β2, β3 or β4. *X. laevis* oocytes were voltage clamped as described in Methods. (A) Representative sodium current traces in response to activation steps, between −50 and 50 mV in 5 mV increments, from a holding potential of −80 mV. (B) activation curves (left, where V_m represents the V_{step} of the test pulse) and inactivation curves (right, where V_m represents the V_{step} of the conditioning prepulse) acquired and plotted as described in Methods. Data points represent mean ± SE, with $n \geq 6$ oocytes. Solid curves are fits of the data to the Boltzmann equation (see Methods), parameters of which are presented in Table 1.

Na$_V$1.7 in our hands are qualitatively consistent with those reported by Chahine's laboratory (Vijayaragavan *et al.*, 2001). Effects of co-expression of the Na$_V$β subunits, particularly the increase in the rate of fast inactivation by Na$_V$β1 and β3, but not by Na$_V$β2 and β4, were also evident with the other three α-subunits, Na$_V$1.1, 1.2 and 1.6, examined in this report (see Supporting Information Table S1).

Na$_V$β subunit co-expression alters the kinetics of block by μ-conotoxins

The effects of co-expression of Na$_V$β1, β2, β3 or β4 on the block of Na$_V$1.7 by μ-SmIIIA are illustrated in Figures 3 and 4. Representative sodium current (I_{Na}) traces are shown in Figure 3A, and representative time courses of block and recovery of from block of peak I_{Na} are shown in Figure 3B and C respectively. Co-expression of Na$_V$β1 and β3 clearly accelerated the block of Na$_V$1.7 by μ-SmIIIA, whereas co-expression of Na$_V$β2 and β4 decelerated the block (Figure 3B). Co-expression of Na$_V$β2 and β4 decreased the rate of dissociation of μ-SmIIIA from Na$_V$1.7, while co-expression of Na$_V$β1 and β3 had minimal effects (Figure 3C).

On-rate constants, k_{on}, were obtained from plots such as those in Figure 3B by fitting the onset of block to a single-exponential function to obtain the observed rate constant, k_{obs}. Plots of k_{obs} versus toxin concentration yielded linear curves (Figure 4A), the slopes of which provided k_{on} values (see Methods) that are listed in Table 2.

Experiments such as those described in Figures 3 and 4 were also performed for Na$_V$1.1, 1.2, 1.6 and 1.7 with μ-conotoxins TIIIA, μ-PIIIA as well as μ-SmIIIA. These results are summarized in Table 2. Note that all three toxins blocked Na$_V$1.1 and 1.2, while Na$_V$1.6 was blocked by μ-SmIIIA and μ-PIIIA but hardly at all by μ-TIIIA; finally, Na$_V$1.7 was blocked only by μ-SmIIIA. The estimated lower-limit K_d values of the impotent blockers are given in the footnotes of Table 2.

A conotoxin that blocks Na$_V$1.7 much like μ-SmIIIA (but more slowly) is μ-KIIIA (Wilson *et al.*, 2011a), so this conopeptide's block of Na$_V$1.7 was also examined for reasons mentioned in the Introduction, and the results are in Table 3.

Co-expression of two chimeras, Na$_V$β112 and Na$_V$β211, constructed from different parts of Na$_V$β1 and Na$_V$β2, and their effects on μ-SmIIIA's block of Na$_V$1.7

These Na$_V$β chimera experiments followed the footsteps of others (e.g. Makita *et al.*, 1996; Zimmer and Benndorf, 2002). To determine which portions of the Na$_V$β subunit (i.e. extra-

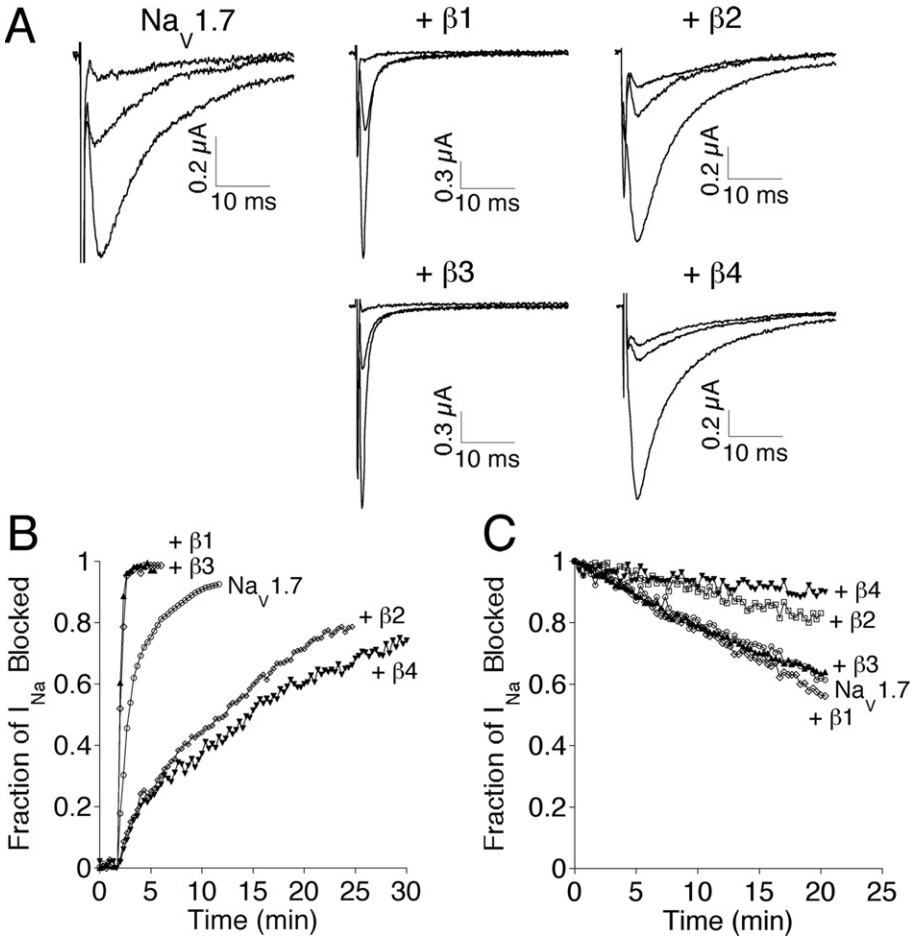

Figure 3

Effects of co-expression of Na$_V$β1, β2, β3, or β4 on the kinetics of block of Na$_V$1.7 by 10 μM μ-SmIIIA. I_{Na} of voltage-clamped oocytes expressing Na$_V$1.7 ± Na$_V$β co-expression was measured as described in Methods. Representative I_{Na} traces (A), time course of block upon exposure to peptide (B) and time course of recovery following peptide washout (C). In panel A, each set of three traces is from a different oocyte: the largest trace represents the control response obtained before exposure to peptide; the smallest trace corresponds to the last response obtained in the presence of peptide in panel B; and the middle trace is the last response obtained during peptide washout in panel C. Each curve in panels B and C is from a different oocyte, where a given symbol represents the co-expression with the same Na$_V$β-subunit in both panels B and C. The observed rate constant of block (k_{obs}) was obtained by fitting curves, such as those in panel B, each to a single exponential; the slope of the plot of k_{obs} as a function of peptide concentration (see Figure 4A) yielded the on rate constant, k_{on}. Values of k_{off} were obtained by measuring the level of recovery at the end of a 20 min wash (e.g. panel C) and assuming recovery followed a single-exponential time course (or, when >50% recovery was achieved within 20 min, by actually fitting the washout curve to a single exponential, see Methods); resulting k_{off} values are provided in Table 2.

cellular, intracellular or transmembrane) were responsible for the subunit's effects, two chimeras of Na$_V$β1 and β2 were constructed and tested: the Na$_V$β112 chimera consisted of Na$_V$β1 with its intracellular portion replaced by that of Na$_V$β2, while the Na$_V$β211 chimera consisted of Na$_V$β1 with its extracellular portion replaced by that of Na$_V$β2 (see Figure 4B). Plotted in Figure 4A are data displaying the consequences of the co-expression of the two chimeras on the susceptibility of Na$_V$1.7 to μ-SmIIIA; the curve representing Na$_V$β112 lies essentially superimposed on those of Na$_V$β1 and β3, while the Na$_V$β211 curve lies near that of Na$_V$β2. The quantified kinetic constants are presented near the bottom of Table 2, which shows that the k_{on} and k_{off} values with Na$_V$β112 co-expression are close to the corresponding rate constants with Na$_V$β1 co-expression; likewise, each rate constant with Na$_V$β211 co-expression is close to that corresponding to Na$_V$β2 co-expression. These results suggest that the extracellular portion of the Na$_V$β subunit is largely responsible for the β-subunit's ability to modulate the susceptibility of Na$_V$1.7 to μ-SmIIIA.

Binary combinations of Na$_V$β subunits co-expressed with Na$_V$1.7: effects on μ-SmIIIA's kinetics

Thus far, we've only considered unary co-expression of Na$_V$β subunits; however, an α-subunit can associate with a binary combination of Na$_V$β subunits [e.g. β1 and β2 (Hartshorne and Catterall, 1984), or one non-covalently (β1 or β3) and one covalently (β2 or β4) (Patino and Isom, 2010)] to form a

Table 2

Influence of the co-expression of rat $Na_V\beta1$, β2, β3 or β4 on the of block of rat $Na_V1.1$, 1.2, 1.6 or 1.7 by μ-TIIIA, μ-PIIIA or μ-SmIIIA[a]

	μ-SmIIIA			μ-PIIIA			μ-TIIIA		
	k_{on} ($\mu M \cdot min)^{-1}$	k_{off} (min^{-1})	K_d (μM)	k_{on} ($\mu M \cdot min)^{-1}$	k_{off} (min^{-1})	K_d or IC_{50}[b] (μM)	k_{on} ($\mu M \cdot min)^{-1}$	k_{off} (min^{-1})	K_d or IC_{50}[b] (μM)
$Na_V1.1$	2.4 ± 0.1	0.009 ± 0.001	0.0038 ± 0.0004	1.0 ± 0.1	0.053 ± 0.003	0.053 ± 0.004	0.39 ± 0.03	1.10 ± 0.22	0.90 ± 0.08[b]
+β1	7.1 ± 1.3	0.017 ± 0.003	0.0024 ± 0.0006	6.1 ± 0.8	0.084 ± 0.006	0.014 ± 0.002	0.49 ± 0.04	0.78 ± 0.14	0.71 ± 0.07[b]
+β2	0.030 ± 0.002	0.0024 ± 0.0003	0.07 ± 0.01	0.044 ± 0.002	0.006 ± 0.001	0.14 ± 0.02	0.35 ± 0.03	1.01 ± 0.08	1.7 ± 0.1[b]
+β3	4.4 ± 0.5	0.010 ± 0.001	0.0023 ± 0.0003	5.20 ± 0.47	0.09 ± 0.01	0.017 ± 0.003	1.96 ± 0.06	0.84 ± 0.09	0.48 ± 0.05[b]
+β4	0.010 ± 0.002	0.0027 ± 0.0006	0.30 ± 0.08	0.019 ± 0.002	0.007 ± 0.002	0.37 ± 0.11	0.14 ± 0.04	0.47 ± 0.05	1.66 ± 0.16[b]
$Na_V1.2$	1.5 ± 0.1	0.0017 ± 0.0004	0.0013 ± 0.0003	0.48 ± 0.04	0.24 ± 0.02	0.62 ± 0.04[b]	0.44 ± 0.02	0.020 ± 0.002	0.045 ± 0.005
+β1	3.5 ± 0.4	0.0028 ± 0.0007	0.0009 ± 0.0002	1.82 ± 0.28	0.16 ± 0.01	0.24 ± 0.03[b]	0.41 ± 0.07	0.016 ± 0.002	0.039 ± 0.008
+β2	0.61 ± 0.06	0.0016 ± 0.0002	0.0030 ± 0.0005	0.21 ± 0.02	0.14 ± 0.02	0.65 ± 0.05[b]	0.49 ± 0.018	0.027 ± 0.003	0.055 ± 0.006
+β3	3.2 ± 0.2	0.0025 ± 0.001	0.0009 ± 0.0003	1.1 ± 0.3	0.20 ± 0.03	0.22 ± 0.02[b]	0.68 ± 0.05	0.009 ± 0.001	0.015 ± 0.002
+β4	0.40 ± 0.04	0.0030 ± 0.0001	0.0075 ± 0.0008	0.17 ± 0.03	0.14 ± 0.01	1.10 ± 0.05[b]	0.21 ± 0.014	0.014 ± 0.002	0.067 ± 0.010
$Na_V1.6$[c]	1.70 ± 0.18	0.12 ± 0.02	0.069 ± 0.013	0.82 ± 0.29	0.067 ± 0.012	0.081 ± 0.032			
+β1	2.38 ± 0.05	0.11 ± 0.01	0.046 ± 0.003	7.77 ± 0.45	0.039 ± 0.006	0.005 ± 0.001			
+β2	0.05 ± 0.00	0.035 ± 0.003	0.75 ± 0.06	0.19 ± 0.04	0.046 ± 0.006	0.243 ± 0.058			
+β3	1.87 ± 0.34	0.11 ± 0.01	0.059 ± 0.013	6.59 ± 0.47	0.062 ± 0.010	0.009 ± 0.002			
+β4	0.030 ± 0.007	0.014 ± 0.003	0.40 ± 0.12	0.18 ± 0.02	0.168 ± 0.015	0.951 ± 0.151			
$Na_V1.7$[d]	0.12 ± 0.01	0.031 ± 0.005	0.26 ± 0.05						
+β1	0.27 ± 0.05	0.034 ± 0.002	0.13 ± 0.02						
+β2	0.010 ± 0.001	0.015 ± 0.002	1.50 ± 0.22						
+β3	0.252 ± 0.017	0.027 ± 0.001	0.11 ± 0.01						
+β4	0.0063 ± 0.0002	0.0067 ± 0.0004	1.17 ± 0.08						
+β112	0.27 ± 0.02	0.027 ± 0.002	0.10 ± 0.01						
+β211	0.015 ± 0.001	0.018 ± 0.003	1.20 ± 0.22						
+β1+β2	0.047 ± 0.010	0.018 ± 0.003	0.38 ± 0.10						
+β1+β4	0.011 ± 0.001	0.0056 ± 0.0004	0.55 ± 0.08						
+β3+β2	0.056 ± 0.008	0.011 ± 0.001	0.20 ± 0.03						
+β3+β4	0.018 ± 0.001	0.0064 ± 0.0004	0.35 ± 0.03						

[a]Values are mean ± SE ($n \geq 9$ oocytes) and were obtained as described in Methods (see also Figure 3); values for $Na_V1.1$, 1.2 and 1.7, all without $Na_V\beta$-subunit co-expression, are from (Wilson *et al.*, 2011a).
[b]Value is K_d, but if it has a superscript 'b', then it is IC_{50} (see Methods).
[c]$Na_V1.6$, regardless of $Na_V\beta$-subunit co-expression, was poorly blocked by μ-TIIIA – at 100 μM, the highest concentration tested, ≲ 30% block was observed in all cases, from which a minimum K_d >200 μM was estimated (see Methods); furthermore, the k_{obs} and k_{off} were too large (>2·min^{-1}) to accurately measure, so corresponding area in table is greyed out.
[d]$Na_V1.7$, regardless of $Na_V\beta$-subunit co-expressed, was essentially insensitive to μ-PIIIA and μ-TIIIA – at 30 μM, the highest concentration tested, each peptide blocked less than 5%, which indicates a minimum K_d > 570 μM, so corresponding areas are greyed out. Plots of k_{obs} versus [μ-conotoxin], the slopes of which provided k_{on} values listed here, are illustrated in Figure 4A and Supporting Information Figure S1.

Table 3

Influence of the co-expression of $Na_V\beta1$, β2, β3 or β4 on the kinetics of block of $Na_V1.7$ by μ-conotoxin KIIIIA[a]

	k_{on} (μM·min)$^{-1}$	k_{off} (min^{-1})	K_d (μM)
$Na_V1.7$	0.024 ± 0.002	0.007 ± 0.001	0.292 ± 0.052
+β1	0.041 ± 0.001*	0.010 ± 0.001*	0.244 ± 0.025
+β2	0.0053 ± 0.0007*	0.0073 ± 0.0011	1.38 ± 0.03
+β3	0.031 ± 0.004	0.013 ± 0.001*	0.42 ± 0.06
+β4	0.0030 ± 0.0002*	0.0027 ± 0.0007*	0.93 ± 0.24

[a]Values are mean ± SE ($n \geq 9$ oocytes). Values for $Na_V1.7$ without any $Na_V\beta$-subunit co-expression are from Wilson *et al.*, (2011a).
*Statistically different than $Na_V1.7$ without $Na_V\beta$-subunit co-expression ($P < 0.05$). Plots of k_{obs} versus [μ-KIIIA], the slopes of which yielded the k_{on} values listed here, are shown in the lower-right corner of Supporting Information Figure S1.

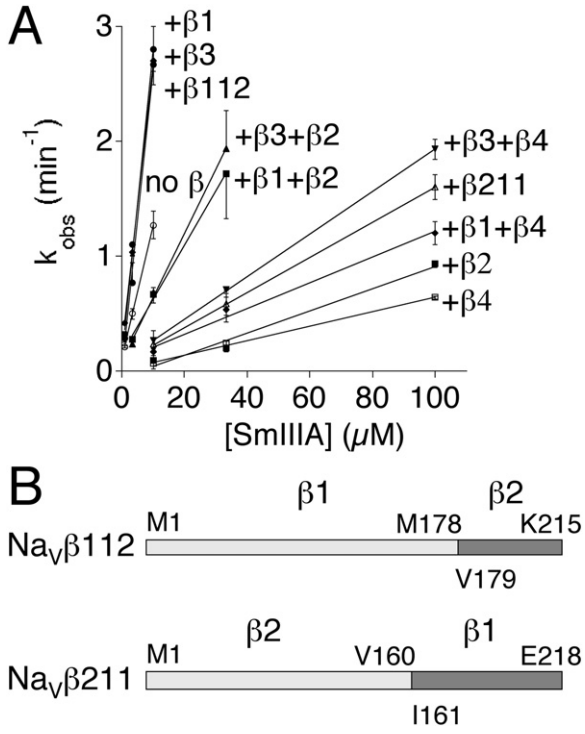

Figure 4

Peptide concentration dependency of the observed rate constants (k_{obs}) for the block by μ-SmIIIA of $Na_V1.7$ either alone, co-expressed with $Na_V\beta1$, β2, β3 or β4 (individually or in pairs) or co-expressed with the chimeras $Na_V\beta112$ or $Na_V\beta211$. Peak I_{Na} of voltage-clamped oocytes expressing $Na_V1.7$ ± co-expression of indicated $Na_V\beta$ subunit(s) were monitored as in Figure 3. (A) The three steepest curves, which essentially overlie each other, are those of $Na_V\beta1$, β3 and the β112 chimera. The remaining curves, in the order of decreasing slope, are those of $Na_V1.7$ alone, +β3 + β2, +β1 + β2, +β3 + β4, +β211 chimera, +β1 + β4, +β2 and +β4. Slopes of curves such as these provided k_{on} values in Table 2. (B) Cartoon of chimeras of $Na_V\beta1$ and $Na_V\beta2$ with amino acid residues at splice sites, as well as at N- and C-termini, indicated. Top, the $Na_V\beta112$ chimera consisted of the extracellular and transmembrane portions of $Na_V\beta1$ and the intracellular portion of $Na_V\beta2$. Bottom, the $Na_V\beta211$ chimera was formed from the extracellular portion of $Na_V\beta2$ and the transmembrane and intracellular portions of $Na_V\beta1$. cRNA encoding these chimeras were made as described in Methods.

ternary complex. We co-expressed $Na_V\beta$ subunits in four binary combinations of $Na_V\beta$ subunits (+β1+β2, +β1+β4, +β3+β2 and +β3+β4) with $Na_V1.7$, and the block by μ-SmIIIA of each combination was assessed. The unary k_{on} value of a given β-subunit of a combination differed from that of its partner by at least an order of magnitude (Table 2); nevertheless, the observed rate of block by μ-SmIIIA of the I_{Na} of oocytes expressing each of the four combinations could be fit by single-exponential functions (not shown), suggesting that in each case a relatively homogeneous population of channels was being expressed. This, in turn, suggests that essentially all the functional channels expressed by given oocyte were likely a ternary complex possessing the same pair of $Na_V\beta$ subunits. The constants for the block of these channels by μ-SmIIIA are presented near the bottom of Table 2 (see also Figure 4A).

Effects of $Na_V\beta$-subunit co-expression on TTX and STX block of $Na_V1.1$ and 1.7

In view of the relatively large decreases in k_{on} produced by co-expression of $Na_V\beta2$ and β4 with $Na_V1.1$ and 1.7 (Table 2) (ranging from >5-fold to 240-fold for at least two μ-conopeptides; see Figure 5 below), we examined whether the block of $Na_V1.1$ and 1.7 by TTX and STX was also affected by $Na_V\beta$ subunit co-expression. The results are presented in Table 4 and summarized as follows. (i) The k_{on} values of TTX for both $Na_V1.1$ and 1.7 were essentially the same. (ii) The k_{off} of TTX for $Na_V1.1$ was about twice that for $Na_V1.7$ and presumably accounts for the twofold difference in the IC_{50} values of TTX for these two Na_V1 isoforms. (iii) The k_{off} values of STX for $Na_V1.1$ and 1.7 were essentially the same. (iv) The k_{on} of STX for $Na_V1.1$ was larger than that for $Na_V1.7$ and presumably largely accounts for the difference in the IC_{50} values of STX for the two Na_V1 isoforms. (v) Overall, $Na_V\beta$ subunit co-expression had no statistically significant effect on the binding properties of TTX and STX, except: (i) $Na_V\beta3$ co-expression slightly elevated the k_{on} of TTX for $Na_V1.1$ (k_{on} was altered by a factor of 1.25); and (ii) $Na_V\beta2$ co-expression slightly reduced the k_{on} of TTX for $Na_V1.7$ (k_{on} was altered by a factor of 0.8). Thus, unlike the binding of μ-conotoxins, the binding of STX and TTX to the channel's pore was only minimally affected by co-expression of the channel with $Na_V\beta$ subunits.

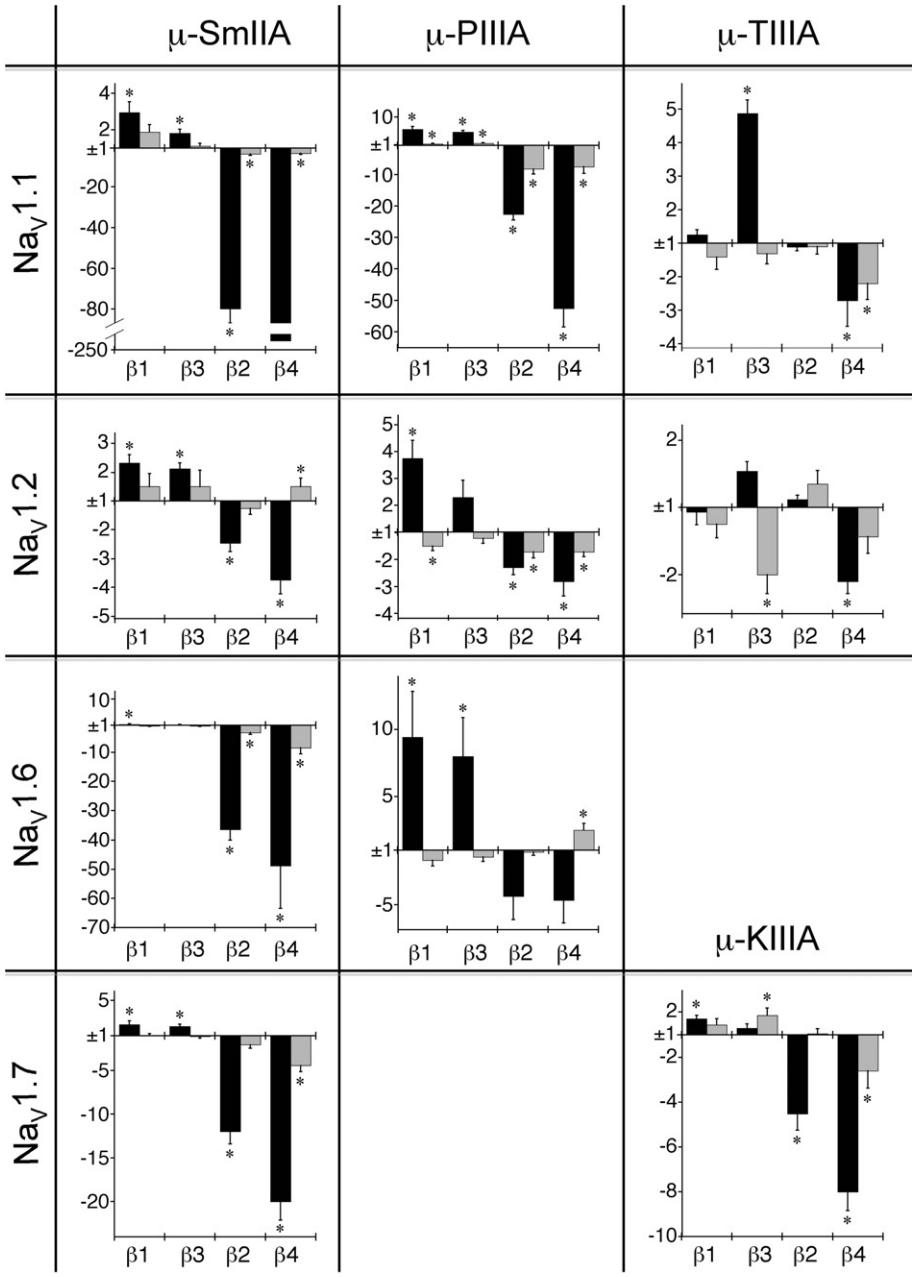

Figure 5

Matrix of plots summarizing the changes in rate constant (Δk) of block by μ-SmIIIA, μ-PIIIA or μ-TIIIA of Na$_V$1.1, 1.2, 1.6 or 1.7 induced by co-expression with Na$_V$β1, β3, β2 or β4. μ-PIIIA and μ-TIIIA don't block Na$_V$1.7, and μ-TIIIA blocks Na$_V$1.6 very poorly, so no results are shown for those combinations; instead, lower right corner shows results for the block by μ-KIIIA of Na$_V$1.7. Bars represent values of Δk_{on} or Δk_{off} (mean ± SE). The *Y*-axis shows the Δk value, where, as described in Methods, an upward (positive-going) bar indicates the factor by which Na$_V$β co-expression increased k, and a downward (negative-going) bar indicates the factor by which Na$_V$β co-expression decreased k. Note, the scale for both directions is the same in a given plot except the first (where the downward bars are shown with a relatively compressed *Y*-axis scale and a break in the plot was necessary to accommodate the very large decrease in k_{on} induced by Na$_V$β4 co-expression (240 ± 49.5, statistically different from Na$_V$1.1 expressed alone, $P < 0.0001$). Values of k_{on} and k_{off} in Tables 2 and 3 were used to calculate Δk values in these plots. *Statistically different from α-subunit expressed alone ($P < 0.05$).

Discussion and conclusions

This report reveals a new way to functionally characterized the interaction of β- with α-subunits of VGSCs. Previously, such interactions were assessed almost exclusively by analyzing how Na$_V$β subunit co-expression modulated the gating of the channel (i.e. the biophysical characteristics and parameters such those as illustrated in Figure 2 and listed Table 1). The ensuing figures and tables in this report clearly demonstrate that β-subunit co-expression in oocytes can alter an

Table 4

Influence of co-expression of $Na_V\beta1$, β2, β3 or β4 on the block of $Na_V1.1$ and $Na_V1.7$ by TTX or STX[a]

	TTX			STX		
	k_{on} ($\mu M \cdot min)^{-1}$	k_{off} (min^{-1})	IC_{50} (nM)	k_{on} ($\mu M \cdot min)^{-1}$	k_{off} (min^{-1})	IC_{50} (nM)
$Na_V1.1$	49.7 ± 4.2	1.17 ± 0.06	13.7 ± 0.6	351.7 ± 27.2	1.50 ± 0.07	2.11 ± 0.06
$Na_V1.1+\beta1$	55.1 ± 7.1	1.18 ± 0.09	13.7 ± 0.6	358.1 ± 22.1	1.39 ± 0.05	2.10 ± 0.06
$Na_V1.1+\beta2$	49.1 ± 7.1	1.40 ± 0.08	13.1 ± 0.5	372.0 ± 21.0	1.38 ± 0.07	2.2 ± 0.1
$Na_V1.1+\beta3$	62.1 ± 1.3*	1.42 ± 0.05	14.0 ± 0.4	320.5 ± 19.2	1.40 ± 0.02	2.26 ± 0.05
$Na_V1.1+\beta4$	53.5 ± 9.6	1.42 ± 0.13	13.4 ± 0.4	433.9 ± 53.5	1.38 ± 0.05	1.99 ± 0.08
$Na_V1.7$	49.6 ± 3.7	0.46 ± 0.04	7.5 ± 0.4	266.8 ± 33.4	1.66 ± 0.18	5.1 ± 0.4
$Na_V1.7+\beta1$	56.6 ± 1.1	0.46 ± 0.04	6.3 ± 0.4	251.0 ± 21.5	1.51 ± 0.07	5.2 ± 0.2
$Na_V1.7+\beta2$	40.0 ± 1.3*	0.38 ± 0.02	7.0 ± 0.3	206.3 ± 9.8	1.42 ± 0.05	4.3 ± 0.2
$Na_V1.7+\beta3$	47.5 ± 1.0	0.42 ± 0.02	6.8 ± 0.3	236.1 ± 25.7	1.47 ± 0.03	5.1 ± 0.3
$Na_V1.7+\beta4$	42.8 ± 2.3	0.44 ± 0.03	7.0 ± 0.4	241.9 ± 40.4	1.38 ± 0.06	4.5 ± 0.3

[a]Values are mean ± SE ($n \geq 9$ oocytes).
*Statistically different than corresponding Na_V1-subunit expressed without any $Na_V\beta$-subunit ($P < 0.03$). Sample current traces of the block by 10 μM TTX, as well as sample time courses for the bock by10 μM TTX and its washout, are illustrated in Supporting Information Figure S2.

α-subunit's susceptibility to μ-conotoxins, but much less so to TTX or STX. We discuss our results here under two headings: (i) consequences of $Na_V\beta$ subunit co-expression on the μ-conotoxin susceptibility of VGSCs and (ii) prospects of using μ-conotoxins to identify the $Na_V\beta$ subunit composition of endogenously expressed VGSCs.

(i) Consequences of $Na_V\beta$ subunit co-expression on a channel's interaction with μ-conotoxin

To help distill the large amount of kinetic data presented in Tables 2 and 3, the changes induced by $Na_V\beta$ subunit co-expression on the value of a kinetic constant, Δk, are plotted in Figure 5. The derivation of Δk is given in Methods and outlined in the legend to Figure 5. Thus, Figure 5 represents a matrix of plots summarizing the changes induced by co-expression of each of the four $Na_V\beta$ subunits on the kinetics of block of the various Na_V1 isoforms by the four μ-conotoxins. For the most part, k_{on} was modestly increased by co-expression of β1 or β3 (e.g. <3-fold with μ-SmIIIA on all Na_V1 isoforms; maximum was ~9-fold, which was achieved with μ-PIIIA on $Na_V1.6$). In contrast, k_{on} could be markedly decreased by co-expression of β2 or β4 (minimally twofold in most instances and >10-fold in four instances: $Na_V1.1$ with μ-SmIIIA and μ-PIIIA, and both $Na_V1.6$ and 1.7 with μ-SmIIIA). Alterations in k_{off} were mostly modest (≲4-fold in most instances with the exception of an ~8-fold decrease observed in three instances: μ-PIIIA on $Na_V1.1$ with $Na_V\beta2$ or β4 and μ-SmIIIA on $Na_V1.6$ with $Na_V\beta4$).

Thus, Figure 5 shows two robust effects were observed for the most part; namely, $Na_V\beta1$ and β3 co-expression increased k_{on}, and $Na_V\beta2$ and β4 co-expression decreased k_{on}, the latter quite strikingly in several instances.

Note that each of the four Na_V1 isoforms examined was susceptible to at least two of the tested μ-conotoxins. Only a minority of the μ-conotoxins discovered thus far are able to block $Na_V1.7$ (Wilson *et al.*, 2011a); and tests with μ-KIIIA, in addition to those with μ-SmIIIA, show that the aforementioned generalizations regarding $Na_V\beta$ subunit co-expression apply to $Na_V1.7$. Of note is that μ-KIIIA has only 16 amino acid residues, six fewer than the other μ-conopeptides examined in this report (Figure 1); and additional tests with KIIIA and its synthetic derivatives (e.g. Zhang *et al.*, 2010b) could reveal what factors, such as steric ones, play a role in the modulatory effect of $Na_V\beta$ subunit co-expression on μ-conotoxin activity.

Binary co-expression of $Na_V\beta$ subunits. The block by μ-SmIIIA of $Na_V1.7$ was also examined in the context of binary co-expression of $Na_V\beta$ subunits. Table 5 recasts the binary co-expression data in Table 2 under the assumption that in a ternary VGSC complex (comprised of one α-subunit and two β-subunits), one of the β-subunits is either $Na_V\beta1$ or β3, and the other either $Na_V\beta2$ or β4. The Δk values for unary $Na_V\beta$ co-expression relative to $Na_V1.7$ alone are shown in the first row of each triplet of rows in Table 5; note that these data are also plotted in the lower left graph in Figure 5. The Δk values for binary relative to unary co-expression are in the remaining rows of Table 5. Note that within each triplet of rows, the respective Δk values are similar (i.e. within about a factor of three of each other). It would appear that the relative changes induced by a given β-subunit's co-expression on k_{on} (a decrease in the case of β2 and β4, and an increase in the case of β1 and β3) and on k_{off} (a decrease in the case of β2 and β4, and minimal change in the case of β1 and β3) are not markedly disturbed by the co-expression of an additional β-subunit.

$Na_V\beta1$: β2 chimeras. The β112 and β211chimeras behaved much like $Na_V\beta1$ and $Na_V\beta2$, respectively (Table 2), consistent with the extracellular domain of the molecule being the

Table 5

Block of Na$_V$1.7 by μSmIIIA: Effects of co-expression of binary combinations of Na$_V$β-subunits relative to unary (or no) co-expression of Na$_V$β-subunits[a]

β-subunit(s) co-expressed[b]	Reference Na$_V$1.7[c]	Δk_{on}[d]	Δk_{off}[d]
+β2	alone	−12.0 ± 1.4	−2.1 ± 0.4
+β2+β1	+β1	−5.7 ± 1.6	−1.9 ± 0.3
+β2+β3	+β3	−4.5 ± 0.7	−2.5 ± 0.3
+β4	alone	−20.0 ± 2.1	−4.4 ± 0.8
+β4+β1	+β1	−24.5 ± 5.1	−5.7 ± 0.5
+β4+β3	+β3	−13.9 ± 1.2	−4.5 ± 0.4
+β1	alone	2.3 ± 0.5	1.1 ± 0.2
+β1+β2	+β2	4.7 ± 1.0	1.2 ± 0.3
+β1+β4	+β4	1.8 ± 0.2	−1.2 ± 0.1
+β3	alone	2.1 ± 0.3	−1.1 ± 0.2
+β3+β2	+β2	5.6 ± 0.9	−1.4 ± 0.2
+β3+β4	+β4	3.0 ± 0.2	−1.2 ± 0.1

[a]Original data are in Table 2.
[b]Terminology as in first column of Table 2 for Na$_V$1.7.
[c]Channel used as reference to calculate Δ*k* values; e.g. Δ*k* values with 'alone' as reference correspond to those of Na$_V$1.7 alone (first row in each triplet of rows), which are also plotted in lower-left graph in Figure 5.
[d]Magnitude and polarity of a value were obtained as described in Methods (and Figure 5 legend) except for cases with binary β-subunit co-expression, where the reference was Na$_V$1.7 co-expressed with the β-subunit indicated in second column.

major factor contributing to its phenotype. This is reminiscent of Na$_V$β1's modulation of the gating kinetics of Na$_V$1.2 and 1.4, where the extracellular domain of the Na$_V$β1 subunit was found to contain the determinant site (Chen and Cannon, 1995; Makita *et al.*, 1996; McCormick *et al.*, 1999; Zimmer and Benndorf, 2002).

Block by TTX and STX. The results in Table 4 clearly show that, unlike the binding of μ-conotoxins, the binding of STX and TTX to the channel's pore seems largely immune to co-expression of the channel with Na$_V$β-subunits. Likewise, in our previous experiments, the block of Na$_V$1.8 by STX was only minimally affected by co-expression of any of the four Na$_V$β subunits – the only significant effects were modest decreases in k_{off} induced by co-expression of Na$_V$β1 and β4 (k_{off} reduced by 30% and 40% respectively) (Wilson *et al.*, 2011b). These results are consistent with biochemical experiments involving tritiated-STX binding to Na$_V$1.2 expressed in Chinese hamster cell lines, which showed that the K_d for STX was not affected by co-expression of Na$_V$β1 (Isom *et al.*, 1995b).

Our recent work showed that TTX/STX can co-occupy site 1 with (at least some) μ-conopeptides and suggested that site 1 might be considered a macrosite (Olivera *et al.*, 1991) consisting of two abutting microsites, one very close to the ion-selectivity filter and accessible to TTX or STX (say, 'site 1a') and the other a more superficial site occupiable by μ-conopeptide (say, 'site 1b') (Zhang *et al.*, 2009; 2010a,b). Thus, with regard to our present results, it appears that the 'reach' of Na$_V$β-subunit co-expression extends to site 1b, but not to site 1a.

Site 1 is in the pore loops (or S5–S6 linkers) of the α-subunit (Cestèle and Catterall, 2000), and Na$_V$β1 is close to these loops insofar as the pore loops of the first and fourth domains of the α-subunit contain important determinants that allow β1 to modulate the gating of the α-subunit (Makita *et al.*, 1996; Catterall, 2000). Our results suggest that the other Na$_V$β subunits may likewise be close to site 1(b).

Other considerations. It should be noted that although it is clear that co-expression of Na$_V$β subunits with the various Na$_V$1 isoforms perturbed the block of VGSCs by μ-conotoxins, we cannot conclude unequivocally that the association of the β- with the α-subunit in the plasma membrane *per se* was responsible for the perturbation. Other possibilities exist; for example, the β-subunit could influence posttranslational modifications, such as glycosylation, of the α-subunit during its synthesis.

Regarding glycosylation of Na$_V$β-subunits themselves, mutation of N-linked glycosylation sites (for sialic acids) of Na$_V$β1 and β2 affect their ability, to varying degrees, to modulate the gating of α-subunits (such as Na$_V$1.2, 1.4, 1.5, and 1.7) expressed in CHO cell lines (Johnson *et al.*, 2004; Johnson and Bennett, 2006). It would be interesting to examine whether Na$_V$β-subunit glycosylation plays a role in the β-subunit's ability to modulate μ-conotoxin binding.

(ii) Prospects of using μ-conotoxins to identify the Na$_V$β subunit composition of endogenously expressed VGSCs

An important point to keep in mind in this regard is that the properties of VGSCs produced by different exogenous expression systems can differ; an example close to home is the following. As noted earlier, the rate of fast inactivation of Na$_V$1.7 co-expressed with either Na$_V$β1 or β3 was faster than that of Na$_V$1.7 expressed alone (Figure 1 and Table 2; see also Vijayaragavan *et al.*, 2001). However, this result was not observed when HEK293 cells served as the expression system; there, co-expression of any Na$_V$β isoform (Na$_V$β1-β4) had no effect on the kinetics of Na$_V$1.7 current (Ho *et al.*, 2012). These investigators also noted that their results with HEK293 cells seemed at odds with the behaviour of TTX-sensitive I_{Na} in small neurons of DRG of mice (presumably mediated at least in part by Na$_V$1.7), where fast inactivation is more rapid in control than in mutant mice where Na$_V$β2 expression was knocked out (Lopez-Santiago *et al.*, 2006). It is becoming increasingly clear that the background cell type in which VGSCs are expressed, neuron versus non-neuronal cell line or even among neurons themselves, can influence the physiological properties of VGSCs (Cummins *et al.*, 2001; Dib-Hajj *et al.*, 2009b).

The issue at hand is how important a role does background cell type play in the pharmacological properties of VGSCs (as opposed to their biophysical properties), specifically regarding the pharmacology of site 1. It remains to be seen whether the effects of Na$_V$β subunit co-expression we

report here for oocytes also apply to neurons. With regard to the latter, experiments seem called for that involve the use of siRNA to knockdown the expression levels of specific $Na_V\beta$ isoforms (Bant and Raman, 2010) or mutant (knockout) mice where specific $Na_V\beta$ subunits are not expressed altogether (Lopez-Santiago *et al.*, 2006).

In the meantime, we are characterizing the μ-conotoxin susceptibility of sodium currents in different cell types of DRG neurons (Zhang *et al.*, 2013), with the expectation that cell type-specific differences that show up might be correlatable with the different levels of transcripts for the various $Na_V\beta$ subunits expressed by the different cell types (e.g. Ho *et al.*, 2012).

Conclusions

Our discovery that $Na_V\beta$ subunit co-expression can affect the affinity of VGSCs for μ-conotoxins provides yet another avenue through which to explore the interaction of μ-conotoxins with site 1, a potentially important drug target for the therapeutic treatment of neurological disorders where VGSCs are implicated, such as epilepsy and neuropathic pain (Catterall, 2012; Waxman, 2012).

Acknowledgements

We thank the following for generously providing rat clones: Prof Alan A Goldin (University of California, Irvine, CA), $Na_V1.1$, $Na_V1.2$, $Na_V\beta1$ and $Na_V\beta2$; Prof Lori L Isom (University of Michigan Medical School, Ann Arbor, MI), $Na_V\beta3$ and $Na_V\beta4$; Prof Gail Mandel (Howard Hughes Medical Institute, Portland, OR), $Na_V1.7$.

This work was supported by the National Institutes of Health grant GM 48677 to GB, BMO, JER and DY.

Conflict of interest

BMO is a cofounder of Cognetix, Inc., and GB is a cofounder of NeuroAdjuvants, Inc.

References

Alexander SPH, Mathie A, Peters JA (2011). Guide to Receptors and Channels (GRAC), 5th edition. Br J Pharmacol 164 (Suppl. 1): S1–S324.

Bant JS, Raman IM (2010). Control of transient, resurgent, and persistent current by open-channel block by Na channel beta4 in cultured cerebellar granule neurons. Proc Natl Acad Sci U S A 107: 12357–12362.

Black JA, Dib-Hajj S, McNabola K, Jeste S, Rizzo MA, Kocsis JD *et al.* (1996). Spinal sensory neurons express multiple sodium channel alpha-subunit mRNAs. Brain Res Mol Brain Res 43: 117–131.

Black JA, Liu S, Tanaka M, Cummins TR, Waxman SG (2004). Changes in the expression of tetrodotoxin-sensitive sodium channels within dorsal root ganglia neurons in inflammatory pain. Pain 108: 237–247.

Brackenbury WJ, Isom LL (2011). Na channel β subunits: overachievers of the ion channel family. Front Pharmacol 2: 53.

Bulaj G, West PJ, Garrett JE, Watkins M, Marsh M, Zhang M-M *et al.* (2005). Novel conotoxins from Conus striatus and Conus kinoshitai selectively block TTX-resistant sodium channels. Biochemistry 44: 7259–7265.

Catterall WA (1980). Neurotoxins that act on voltage-sensitive sodium channels in excitable membranes. Annu Rev Pharmacol Toxicol 20: 15–43.

Catterall WA (2000). From ionic currents to molecular mechanisms: the structure and function of voltage-gated sodium channels. Neuron 26: 13–25.

Catterall WA (2012). Voltage-gated sodium channels at 60: structure, function, and pathophysiology. J Physiol 590: 2577–2589.

Catterall WA, Goldin AL, Waxman SG (2005). International Union of Pharmacology. XLVII. Nomenclature and structure-function relationships of voltage-gated sodium channels. Pharmacol Rev 57: 397–409.

Cestèle S, Catterall WA (2000). Molecular mechanisms of neurotoxin action on voltage-gated sodium channels. Biochimie 82: 883–892.

Chahine M, O'leary ME (2011). Regulatory role of voltage-gated Na channel β subunits in sensory neurons. Front Pharmacol 2: 70.

Chen C, Cannon SC (1995). Modulation of Na+ channel inactivation by the beta 1 subunit: a deletion analysis. Pflugers Arch 431: 186–195.

Chopra SS, Watanabe H, Zhong TP, Roden DM (2007). Molecular cloning and analysis of zebrafish voltage-gated sodium channel beta subunit genes: implications for the evolution of electrical signaling in vertebrates. BMC Evol Biol 7: 113.

Cummins TR, Aglieco F, Renganathan M, Herzog RI, Dib-Hajj SD, Waxman SG (2001). Nav1.3 sodium channels: rapid repriming and slow closed-state inactivation display quantitative differences after expression in a mammalian cell line and in spinal sensory neurons. J Neurosci 21: 5952–5961.

Dib-Hajj SD, Black JA, Waxman SG (2009a). Voltage-gated sodium channels: therapeutic targets for pain. Pain Med 10: 1260–1269.

Dib-Hajj SD, Choi J-S, Macala LJ, Tyrrell L, Black JA, Cummins TR *et al.* (2009b). Transfection of rat or mouse neurons by biolistics or electroporation. Nat Protoc 4: 1118–1126.

Dib-Hajj SD, Cummins TR, Waxman SG (2010). Sodium channels in normal and pathological pain. Neuroscience 33: 325–347.

Fiedler B, Zhang M-M, Buczek O, Azam L, Bulaj G, Norton RS *et al.* (2008). Specificity, affinity and efficacy of iota-conotoxin RXIA, an agonist of voltage-gated sodium channels Na(V)1.2, 1.6 and 1.7. Biochem Pharmacol 75: 2334–2344.

Fukuoka T, Kobayashi K, Yamanaka H, Obata K, Dai Y, Noguchi K (2008). Comparative study of the distribution of the alpha-subunits of voltage-gated sodium channels in normal and axotomized rat dorsal root ganglion neurons. J Comp Neurol 510: 188–206.

Hartshorne RP, Catterall WA (1984). The sodium channel from rat brain. Purification and subunit composition. J Biol Chem 259: 1667–1675.

Ho C, Zhao J, Malinoswki S, Chahine M, O'Leary ME (2012). Differential expression of sodium channel β subunits in dorsal root ganglion sensory neurons. J Biol Chem 287: 15044–15053.

Isom LL, De Jongh KS, Patton DE, Reber BF, Offord J, Charbonneau H *et al.* (1992). Primary structure and functional expression of the beta 1 subunit of the rat brain sodium channel. Science 256: 839–842.

Isom LL, Ragsdale DS, De Jongh KS, Westenbroek RE, Reber BF, Scheuer T *et al.* (1995a). Structure and function of the beta 2 subunit of brain sodium channels, a transmembrane glycoprotein with a CAM motif. Cell 83: 433–442.

Isom LL, Scheuer T, Brownstein AB, Ragsdale DS, Murphy BJ, Catterall WA (1995b). Functional co-expression of the beta 1 and type IIA alpha subunits of sodium channels in a mammalian cell line. J Biol Chem 270: 3306–3312.

Johnson D, Bennett ES (2006). Isoform-specific effects of the beta2 subunit on voltage-gated sodium channel gating. J Biol Chem 281: 25875–25881.

Johnson D, Montpetit ML, Stocker PJ, Bennett ES (2004). The sialic acid component of the beta1 subunit modulates voltage-gated sodium channel function. J Biol Chem 279: 44303–44310.

Kilkenny C, Browne W, Cuthill IC, Emerson M, Altman DG (2010). NC3Rs Reporting Guidelines Working Group. Br J Pharmacol 160: 1577–1579.

Lewis RJ, Schroeder CI, Ekberg J, Nielsen KJ, Loughnan M, Thomas L *et al.* (2007). Isolation and structure-activity of mu-conotoxin TIIIA, a potent inhibitor of tetrodotoxin-sensitive voltage-gated sodium channels. Mol Pharmacol 71: 676–685.

Lewis RJ, Dutertre S, Vetter I, Christie MJ (2012). Conus venom Peptide pharmacology. Pharmacol Rev 64: 259–298.

Liman ER, Tytgat J, Hess P (1992). Subunit stoichiometry of a mammalian K+ channel determined by construction of multimeric cDNAs. Neuron 9: 861–871.

Lopez-Santiago LF, Pertin M, Morisod X, Chen C, Hong S, Wiley J *et al.* (2006). Sodium channel beta2 subunits regulate tetrodotoxin-sensitive sodium channels in small dorsal root ganglion neurons and modulate the response to pain. J Neurosci 26: 7984–7994.

Lopreato GF, Lu Y, Southwell A, Atkinson NS, Hillis DM, Wilcox TP *et al.* (2001). Evolution and divergence of sodium channel genes in vertebrates. Proc Natl Acad Sci U S A 98: 7588–7592.

McCormick KA, Srinivasan J, White K, Scheuer T, Catterall WA (1999). The extracellular domain of the beta1 subunit is both necessary and sufficient for beta1-like modulation of sodium channel gating. J Biol Chem 274: 32638–32646.

McGrath J, Drummond G, Kilkenny C, Wainwright C (2010). Guidelines for reporting experiments involving animals: the ARRIVE guidelines. Br J Pharmacol 160: 1573–1576.

Makita N, Bennett PB, George AL (1996). Molecular determinants of beta 1 subunit-induced gating modulation in voltage-dependent Na+ channels. J Neurosci 16: 7117–7127.

Morgan K, Stevens EB, Shah B, Cox PJ, Dixon AK, Lee K *et al.* (2000). beta 3: an additional auxiliary subunit of the voltage-sensitive sodium channel that modulates channel gating with distinct kinetics. Proc Natl Acad Sci U S A 97: 2308–2313.

Olivera BM, Rivier J, Scott JK, Hillyard DR, Cruz LJ (1991). Conotoxins. J Biol Chem 266: 22067–22070.

Patino GA, Isom LL (2010). Electrophysiology and beyond: multiple roles of Na+ channel β subunits in development and disease. Neurosci Lett 486: 53–59.

Rush AM, Cummins TR, Waxman SG (2007). Multiple sodium channels and their roles in electrogenesis within dorsal root ganglion neurons. J Physiol 579 (Pt 1): 1–14.

Shon KJ, Olivera BM, Watkins M, Jacobsen RB, Gray WR, Floresca CZ *et al.* (1998). mu-Conotoxin PIIIA, a new peptide for discriminating among tetrodotoxin-sensitive Na channel subtypes. J Neurosci 18: 4473–4481.

Terlau H, Olivera BM (2004). Conus venoms: a rich source of novel ion channel-targeted peptides. Physiol Rev 84: 41–68.

Vijayaragavan K, O'Leary ME, Chahine M (2001). Gating properties of Na(v)1.7 and Na(v)1.8 peripheral nerve sodium channels. J Neurosci 21: 7909–7918.

Waxman SG (2012). Sodium channels, the electrogenisome, and the electrogenistat: lessons and questions from the clinic. J Physiol 590: 2601–2612.

West PJ, Bulaj G, Garrett JE, Olivera BM, Yoshikami D (2002). Mu-conotoxin SmIIIA, a potent inhibitor of tetrodotoxin-resistant sodium channels in amphibian sympathetic and sensory neurons. Biochemistry 41: 15388–15393.

Widmark J, Sundström G, Ocampo Daza D, Larhammar D (2011). Differential evolution of voltage-gated sodium channels in tetrapods and teleost fishes. Mol Biol Evol 28: 859–871.

Wilson MJ, Yoshikami D, Azam L, Gajewiak J, Olivera BM, Bulaj G *et al.* (2011a). μ-Conotoxins that differentially block sodium channels NaV1.1 through 1.8 identify those responsible for action potentials in sciatic nerve. Proc Natl Acad Sci U S A 108: 10302–10307.

Wilson MJ, Zhang M-M, Azam L, Olivera BM, Bulaj G, Yoshikami D (2011b). Navβ subunits modulate the inhibition of Nav1.8 by the analgesic gating modifier μO-conotoxin MrVIB. J Pharmacol Exp Ther 338: 687–693.

Yu FH, Westenbroek RE, Silos-Santiago I, McCormick KA, Lawson D, Ge P *et al.* (2003). Sodium channel beta4, a new disulfide-linked auxiliary subunit with similarity to beta2. J Neurosci 23: 7577–7585.

Zhang M-M, McArthur JR, Azam L, Bulaj G, Olivera BM, French RJ *et al.* (2009). Synergistic and antagonistic interactions between tetrodotoxin and mu-conotoxin in blocking voltage-gated sodium channels. Channels (Austin, Tex) 3: 32–38.

Zhang M-M, Gruszczynski P, Walewska A, Bulaj G, Olivera BM, Yoshikami D (2010a). Cooccupancy of the outer vestibule of voltage-gated sodium channels by micro-conotoxin KIIIA and saxitoxin or tetrodotoxin. J Neurophysiol 104: 88–97.

Zhang M-M, Han TS, Olivera BM, Bulaj G, Yoshikami D (2010b). μ-conotoxin KIIIA derivatives with divergent affinities versus efficacies in blocking voltage-gated sodium channels. Biochemistry 49: 4804–4812.

Zhang M-M, Wilson MJ, Gajewiak J, Rivier JE, Bulaj G, Olivera BM *et al.* (2013). Pharmacological Fractionation of Tetrodotoxin-sensitive Sodium Currents in Rat Dorsal Root Ganglion Neurons by μ-Conotoxins. Br J Pharmacol. DOI: 10.1111/bph.12119

Zimmer T, Benndorf K (2002). The human heart and rat brain IIA Na+ channels interact with different molecular regions of the beta1 subunit. J Gen Physiol 120: 887–895.

Supporting information

Additional Supporting Information may be found in the online version of this article at the publisher's web-site:

Figure S1 Matrix of k_{obs} versus [μ-conotoxin] plots for the block by μ-SmIIIA, μ-PIIIA or μ-TIIIA of $Na_V1.1$, 1.2, 1.6, or 1.7, each alone or co-expressed with $Na_V\beta1$, β3, β2 or β4. Also included is the plot for the block by μ-KIIIA of $Na_V1.7$ ± $Na_V\beta$-subunits (lower right). Slopes of these plots provided

the k_{on} values for Tables 2 and 3 (and thus the Δk_{on} values in Figure 5). Each plot is modelled after Figure 4A, and overall arrangement of plots mirrors that of Figure 5 (including plot in lower right corner illustrating the results for the block by μ-KIIIA of $Na_V1.7 \pm Na_V\beta$ subunit co-expression). Thus, columns represent different μ-conotoxins, and rows represent different Na_V1 isoforms. Each plot shows five curves: respective Na_V1 alone ('no β'), Na_V1 + β1 ('+β1'), Na_V1 + β2 ('+β2'), Na_V1 + β3 ('+β3') and Na_V1 + β4 ('+β4'). Note, first two plots in the first row and first plot in the third row each have an inset showing curves for 'no β', '+β1' and '+β3' (because these three curves are too close together to easily distinguish among them in the parent plot), where the *X*-axis has been expanded relative to that of the parent plot; the axes of each inset have the same units as those of the parent plot.

Figure S2 Block by TTX of $Na_V1.7$ without (left column) and with co-expression of $Na_V\beta1$ (middle column) or $Na_V\beta4$ (right column). Top row, sample current traces before (control) and during exposure to 10 nM TTX; in each case, the current was blocked by about 60%. Bottom row, representative time courses of block by 10 nM TTX and recovery following TTX washout. Horizontal black bar represents time interval during which TTX was present. Solid curves represent best fits to single-exponential functions, from which values of k_{obs} and k_{off} were obtained. Such k_{off} values from ≥9 oocytes were averaged to yield each k_{off} value in Table 4. Also, such k_{obs} values from 9 oocytes were plotted versus [TTX], and the resulting slope yielded each k_{on} value in Table 4.

Table S1 Time constant of fast inactivation, τ, for $Na_V1.1$, 1.2 and 1.6 without and with co-expression of $Na_V\beta$-subunits.[a]